Model Predictive Control to Maximize the Efficiency in EV Wireless Chargers

Jose M. González-González, Alicia Triviño-Cabrera, José A. Aguado, *Member, IEEE*

***Abstract*—The automotive industry is undergoing a transition towards cleaner and more efficient technologies. Electric Vehicles (EVs) play a relevant role in this scenario. However, these vehicles continue to suffer from limitations in terms of autonomy and charging times, which can be alleviated with wireless charging technology. This technology facilitates the charging process but has a lower efficiency when compared with conductive chargers. This effect is particularly severe under misalignment conditions and with the usual variations of the battery's electrical features. In order to avoid this disadvantage, this paper presents a predictive control algorithm focused on maximizing the charging efficiency. As a novelty, the algorithm sets three configuration parameters in the power converters of the system. The main advantage lies in the fact that it does not need constant monitoring and offers very low response times. This control also improves compatibility with different automobile manufacturers, adding the capacity to work with receivers and batteries with diverse characteristics while complying with international standards. The validity of the proposal is verified by theoretical analysis, simulations and the experimental results of a 2-kW prototype. The results show the feasibility of the proposed control and the improvement in the efficiency of the system.**

***Index Terms*—magnetic resonant coupling, wireless power transfer, electric vehicle, predictive control, energy efficiency.**

NOTATION

Index and sets

i	Index and set for each side of the charger, where 1 is used for primary or transmitter side and 2 is used for secondary or receiver side.

Parameters

C_i	Capacitor value of compensation network [F].
C_{oss}	MOSFET output capacitance [F].
C_{sn}	Capacitor value of snubber [F].
L_i	Coil self-inductance [H].
M	Mutual inductance [H].
$\overline{\omega}$	Maximum angular frequency allowed [rad/s].
$\underline{\omega}$	Minimum angular frequency allowed [rad/s].
P_{ch}	Reference charging power [W].
R_d	Diode resistance [Ω].
R_i	Coil resistance [Ω].
$R_{m,ds}$	MOSFET drain-source on resistance [Ω].
R_{sn}	Resistor value of snubber [Ω].
t_m	MOSFET rise and fall mean time [s].
V_{DC}	Primary DC bus voltage. Maximum voltage in primary side [V].
V_{max}	Maximum input voltage [V].

Variables

ii_i	Imaginary part of the current [A].
ir_i	Real part of the current [A].
V_1	Primary inverter output voltage [V].

Positive variables

α	Phase-shift angle between the switching of both legs of the inverter [rad].
α_{sn}	Correction term for snubber losses [-].
D	Duty cycle of the DC/DC converter [-].
η	Efficiency [-].
im_i	Absolute value of current [A].
L_d	Diode losses [W].
L_m	MOSFET losses [W].
$L_{m,c}$	MOSFET conduction losses [W].
$L_{m,dt}$	MOSFET duty-cycle losses [W].
$L_{m,sn}$	MOSFET snubber losses [W].
$L_{m,sw}$	MOSFET switching losses [W].
ω	Angular frequency $[rad/s]$.
R_{eq}	Equivalent load resistance (in AC side) [Ω].
R_l	Equivalent load resistance (in AC side) [Ω].
V_{in}	Input voltage $[V]$.

Manuscript received Month xx, 2xxx; revised Month xx, xxxx; accepted Month x, xxxx. This work was supported in part by the Spanish Ministerio de Ciencia e Innovacion (MICINN) project PID2019-110531-RA-I00 from the "Proyectos de I+D+i - RTI Tipo A" program

Authors are with the Department of Electrical Engineering, Escuela de Ingenierías Industriales, University of Málaga, Málaga, 29071 Spain (e-mail: josemanuelgonzalez@uma.es.).

I. INTRODUCTION

THE automotive industry is in full transition to more efficient and less polluting technologies [1]. Electric Vehicles (EVs) will play a fundamental role in this evolution with a fleet that is expected to exceed 8.5 million vehicles in 2020 [2]. Although EV technology has significantly evolved in terms of battery capacity and charging times, the autonomy of this kind of vehicle still constitutes a clear limitation. This is the main reason why the penetration rate of EVs is still low according to [3].

Wireless charging, in particular charging based on Magnetic Resonant Coupling (MRC) technology [4], can help promoting the use of EVs. MRC-based wireless chargers for EVs facilitate the charge process with minimal intervention from the driver, even when the vehicle is moving [5]. This kind of charger relies on an air-cored transformer in which two coils are magnetically coupled. The first coil (referred to as the primary coil) is placed on the pavement. It is electrically powered to generate a time-varying magnetic field [6]. When this magnetic field traverses the secondary coil (located in the vehicle's chassis), a voltage is induced. This simple process is enhanced by the inclusion of compensation networks and power converters, which make the power transfer more efficient [4]. Fig. 1 shows a generic diagram for MRC wireless chargers, where L_1 and R_1 define the electrical parameters of the primary coil, L_2 and R_2 the electrical parameters of the secondary coil and M corresponds to the mutual inductance between the two coils. The primary side is equipped with a rectifier and an inverter to force the system to work at high frequencies. In this way, the power transfer is increased. As the battery requires Direct Current (DC), the secondary side depends on a rectifier. In some designs, a DC/DC converter is also incorporated on the secondary side to adjust the voltage to the battery requirements. In this way, the charger is compatible with more types of batteries as the DC/DC converter operates as an impedance adapter and voltage adapter [7].

One key component of the wireless charger is the controller of the power converters. Firstly, the controller must ensure that the battery is charged according to the mode (power level) it requires. In addition to the charging mode, this kind of charger should operate in a wide range of conditions. Specifically, the technical specification IEC TS 61980-3:2019 [8], the standard ISO 19363:2020 [9] and the standard SAE J2954 [10] define the potential characteristics of the chargers. The last document regulates several design aspects of the charger such as coil characteristics, the interval of the valid gap between the coils, the allowed misalignments and the range of the operating frequency. According to this standard, the secondary coil ground clearance range must be between 100 and 250 mm (depending on Z classification) and the frequency should be set in the interval between 81.39 and 90 kHz. The same range for the operation frequency is defined in IEC 61980-3:2019 and ISO 19363:2020. Due to this variety of operation modes, the controllers must adapt the configuration of the power converters. Ignoring the effects of working under conditions different from those assumed in the design process could lead to severe risks [11]. When working with medium power levels, it is crucial to maximize the efficiency of the power transfer. Consequently, this a common goal set in the design of EV wireless chargers [12] and the associated controllers [13].

Setting the goal of maximizing the efficiency, controllers can be broadly divided into two main groups: the ones that tune the operation frequency [14]–[16] and those that operate on the DC/DC converters [13], [17], [18]. However, the optimum efficiency cannot be achieved with the configuration of just one power converter but with the adjustment of both simultaneously [19]. Additionally, these controllers should allow a wide range of potential values for their configuration parameters. Model Predictive Control (MPC) has been recently applied to EV chargers as it has revealed itself as an effective mechanism to search the optimum value in a real interval, without the need for its discretization [20]. Fast response and avoidance of disturbances are also relevant benefits associated to MPC.

This paper proposes a novel MPC, which maximizes the transfer efficiency while at the same time approximating the power delivered to the battery to the target value. In addition to the benefits of using a MPC controller, it also provides the mathematical framework to adjust the DC/DC converter, the operational frequency and the phase shifting simultaneously. The main novelties of the controller are:

- The proposed algorithm aims to maximize the compatibility of the wireless power source with different EV batteries while also increasing the robustness under non-nominal operations such as those caused by misalignments. For this, mutual inductance (M) is dynamically checked.
- The goal of the system is to deliver the required power at the maximum possible efficiency. This could mean that the system may not operate with maximum efficiency to guarantee the reference charging power.
- The control adjusts three parameters: (i) the phase-shifting of the primary converter, (ii) the equivalent impedance of the battery by the duty cycle of the secondary DC/DC converter and (iii) the frequency operation in the range allowed in the RP SAE J2954. By including a secondary DC/DC converter, the system gains compatibility to work with batteries from different manufacturers and requirements. The optimization problem provides a solution with the adequate values of these three parameters. Then, the controller adjusts the power converters concurrently so there is no need to set a priority about which parameters should be set first.
- It is based on one model predictive control to conveniently configure the power converters. The predictive model is used with an optimization algorithm, which avoids the granularity of the tracking control algorithms. It is also able to provide the optimum value for the three configuration parameters altogether.

The control algorithm has been implemented in a 2-kW prototype. The experiments have revealed that the algorithm is able to tune the power converters conveniently for variations in the equivalent resistance and on the mutual inductance. Specifically, the results show that it is more convenient to use three parameters for the adjustment of the system operation according to the set goal.

The paper is organized as follows: Section III presents the selected topology for the development and its theoretical analysis. Section IV defines the design of the proposed control. Section V describes the physical implementation of the MRC WPT and presents the results of the implementation. Finally, Section VI concludes the paper and draws the main conclusions.

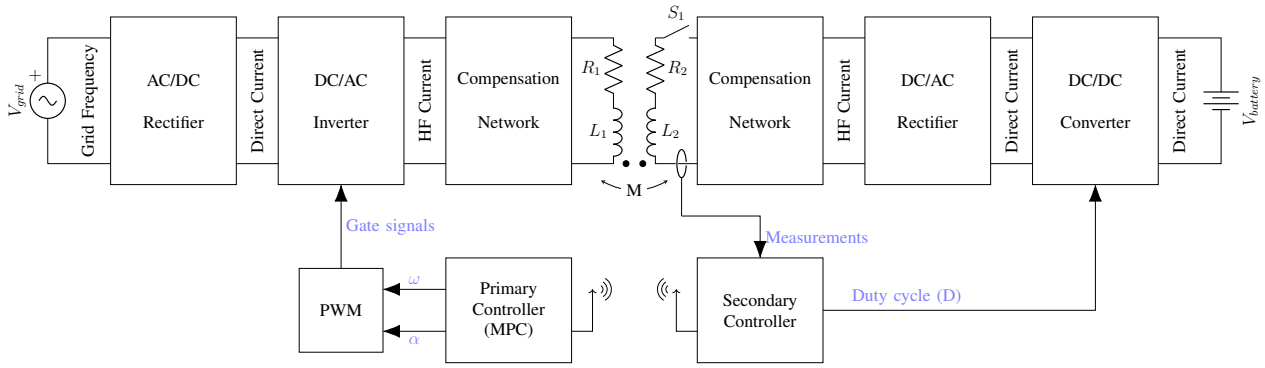

Fig. 1. Generic diagram of the proposed charger.

II. Related work

EV controllers are an essential component of EV wireless chargers as they ensure their proper operation. They are designed to meet multiple objectives. Indeed, there are controllers that have a Constant Power (CP) charging mode [21] and others that allow for a bi-directional power flow [22]. For electric cars, in addition to these goals there is always the requirement of operating at maximum efficiency due to the amount of transferred power. In this context, the proposed controllers can be classified in two main groups: (i) those based on one or two DC/DC converters and (ii) those relying on the frequency adjustment. With regard to the first group, the authors in [13] implement a Maximum Efficiency Point Tracking (MEPT) Control Scheme for a WPT system. The controller operates at a fixed frequency but regulates two DC/DC converters (one on the primary and another on the secondary side) to regulate the voltage input and the reflected impedance. To set the duty cycles of the DC/DC converters, the algorithm applies small disturbances to these variables maintaining a constant output voltage. It then checks whether the efficiency of the system improves. If not, it applies the disturbance in the opposite direction, seeking the best efficiency value. This maximum-efficiency tracking method is a slow process that may not lead to an optimal configuration, as it depends on the additional disturbances step and the accuracy of the measurements. The work in [17] adjusts a secondary DC/DC converter to further maximize the efficiency. It uses a PI-controller to generate the PWM signal. In [18], the authors seek the maximum efficiency point by regulating a switching voltage regulator on the secondary side. The work in [23] demonstrates the convenience of dynamically estimating the coupling coefficient to improve the power transfer efficiency tracking. In this way, the controller is able to adjust the duty cycle of the primary and secondary DC/DC power converters to the variations in the coupling coefficient.

The previous systems work with a fixed frequency, even though the frequency is a value that impacts on the efficiency of the power transfer [24]. Under ideal conditions, the operating frequency of an EV wireless charger matches the resonant frequency to optimize the power transfer and the efficiency [25]. However, the components are manufactured with a tolerance margin which implies that their values differ from the nominal ones. As a result, the operation frequency may not be equal to the resonant frequency considered in the design. To cope with this issue, the authors in [14], [15] propose a frequency-tracking algorithm for low power and high frequency MRC system. With an iterative algorithm, the control tests several frequencies to detect the value that provides the highest efficiency. This proposal is improved in [16], in which the implemented algorithm aims to minimize the input power by varying both the frequency and phase shift of the primary inverter. In these control algorithms, the parameter to adjust (frequency or phase shifting) can only be set to an item in a range of potential values defined previously. To extend the values for these parameters, predictive strategies can be used, leading to better adjustments [26], [27].

Model Predictive Control (MPC) is a technique that relies on a mathematical model to predict future behavior of a system so that it obtains the optimum configuration of the system in order to meet an objective. MPC repeats the optimization calculations on line without restricting the potential values of the configuration parameters to a set. Once it finds the optimum configuration, the controller adjusts the power converters accordingly and simultaneously [28]. This control technique offers many benefits [29] such as the ability to be used in a wide variety of systems, and the possibility to easily include non-linearities and restrictions in the objective function. When compared to a proportional integral differential PID control, MPC is faster and it can effectively overcome the influences of disturbances [20]. For an EV wireless charger, these features are convenient when it is necessary to solve a multivariable optimization problem. Specifically, the search for optimum efficiency is a problem that depends on the parameters of the power converters (frequency, phase shifting and/or duty cycle).

One of the most relevant predictive controls applied to wireless charging can be found in [30]. The authors develop a bi-layer control for bi-directional chargers. The algorithm decides the amount of power to transfer by taking into account the battery state, the driver's preference and the prices. Then, the algorithm decides the configuration parameters of the primary power converter. In their design, the DC/DC converter is not included on the secondary side and the operating frequency is kept constant. The work in [31] uses a MPC to decide the amount of power to deliver to the battery by adjusting the primary inverter only. The work in [20] also uses a MPC

algorithm. Specifically, it configures the DC/DC converter on the secondary side of a dynamic wireless charging system. The results demonstrate that the MPC is able to reduce the response time and its variability when compared with a PID controller. The work in [32] realises that the maximum efficiency requires the configuration of more than one power converter. The authors propose the use of two independent MPC, one for the primary inverter and another for the secondary controlled rectifier. The results are the local optimum values for the phase shifting of the primary inverter and the secondary rectifier. A non-trivial coordination is proposed to prioritize which parameter should be set first.

It can be observed that MPC has been applied to EV wireless charger but just to control one power converter. Our proposal aims at properly configuring two power converters and three configuration parameters with only one MPC. The use of one MPC avoids deciding which parameter should be set first as all of them are configured concurrently.

III. Circuit analysis

The configuration of the power converters and the topology of the compensation networks restrict where and how the control algorithms can be applied. With regard to the matching networks, although the multi-resonant topologies have shown their ability to cope with misalignment and avoid the bifurcation problem [4], the Series-Series (SS) compensation network leads to a lower amount of losses when the system is properly configured [33]. This is the reason why the feasibility of the proposed control algorithm has been analyzed with a Series-Series compensation network. However, its application is also valid in other topologies once some equations of the algorithm are modified. For a Series-Series compensation topology, the values of the capacitors are related to the inductances and the nominal frequency. Thus:

$$C_1 = \frac{1}{\omega_o^2 L_1}; \qquad C_2 = \frac{1}{\omega_o^2 L_2} \tag{1}$$

where ω_o is the design angular frequency $[rad/s]$, C_1 and C_2 are the compensation capacitance and L_1 and L_2 the coil inductance of the primary side and secondary sides respectively.

Assuming a first harmonic approximation, the output of the primary inverter can be modelled as a sine-wave source. This simplification leads to the circuit depicted in Figure 2.

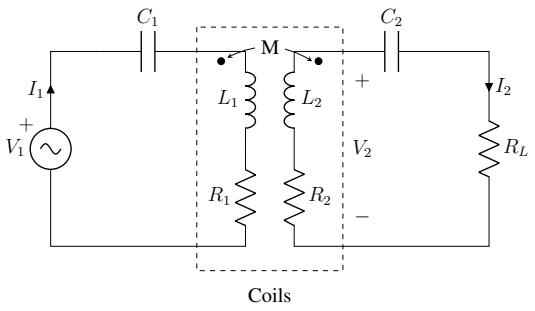

Fig. 2. Generic diagram for magnetic resonance wireless chargers with SS compensation networks.

In this circuit, we have that:

$$V_1 = \left(R_1 + j\omega L_1 - \frac{j}{\omega C_1}\right) I_1 + j\omega M I_2 \tag{2}$$

$$0 = j\omega M I_1 + \left(R_2 + R_L + j\omega L_2 - \frac{j}{\omega C_2}\right) I_2 \tag{3}$$

where V_1 is the voltage of the primary side, I_1 and I_2 are the currents flowing through the primary and secondary side respectively, M is the mutual inductance, R_L is the load resistance and ω is the frequency. As V_1 is the output of the primary inverter, a Phase Shifting Modulation (PSM) can be applied to adjust its value. In particular:

$$V_1 = \frac{2\sqrt{2}V_{in}}{\pi} \sin\frac{\alpha}{2} \tag{4}$$

where V_{in} is the DC input voltage and α a parameter which defines the phase shift between the switching of both legs of the inverter.

The secondary DC/DC converter allows regulating the voltage and the charging power delivered to the battery. To do so, it also alters the value of the equivalent resistance of the battery perceived by the rest of the system. Its effect depends on the type of converter implemented. As we demonstrate in Section IV, lower values of the equivalent resistance increase the efficiency of the charger. Since the boost converter is able to reduce the equivalent impedance, it has been selected for the proposed charger. For this DC/DC converter, and assuming a Continuous Current Mode, the load resistance (R_L) of the battery is defined as:

$$R_L = (1 - D)^2 R_{batt} \tag{5}$$

where D is the Duty Cycle of the DC/DC converter and R_{batt} is the equivalent resistance of the battery, which can be determined with the battery voltage V_{batt} and its charging power P_{ch}. Thus, $R_{batt} = \frac{V_{batt}^2}{P_{ch}}$.

The battery can be modelled as an equivalent resistance (R_{eq}) including the effects of the secondary rectifier. The resulting value is:

$$R_{eq} = \frac{8R_L}{\pi^2} \tag{6}$$

The theoretical efficiency (η_{th}) of the system is thus defined as:

$$\eta_{th} = \frac{R_{eq}}{R_1\left(\frac{R_2+R_{eq}}{\omega M}\right)^2 + R_2 + R_{eq}} \tag{7}$$

A wireless charger must be efficient but it must also deliver the required charging power (P_{ch}) to the battery. In particular, for the system, this value corresponds to:

$$P_{ch} = \left|\frac{j\omega M I_1}{R_2 + R_{eq} + j\omega L_2}\right|^2 R_{eq} \tag{8}$$

With the inclusion of a DC / DC converter in the charger, there are three operating points that can be adjusted to optimize the efficiency of the charging process: (i) the frequency ω of

the inverter; (ii) the rms of the output voltage of the inverter, controlled by the PSM with the α parameter; and (iii) the duty cycle D of the DC/DC converter on the secondary side. The configuration of the phase shift α varies the power delivered to the load. Alternatively, the effects of tuning the frequency and adjusting the R_{eq} are notorious in terms of efficiency. Fig. 3 shows the evolution of the efficiency for different values of R_{eq} and frequency in a charger with the features summarized in Table I. As expressed in (7), these functions are independent of the α parameter. The maximum efficiency value is reached on the blue curve, corresponding to an operating frequency of 82 kHz and a R_{eq} of 7 Ω. It is observed that lower load resistances lead to better efficiencies. It can be observed that for lower frequencies, the resistance with which the maximum efficiency point is reached drops. The highest efficiencies are achieved with lower frequencies. The difference between the maximum efficiency points of the different frequencies allowed in the RP SAE J2954 reaches 1%, although this value increases as the R_{eq} moves away from the maximum efficiency point. The value of R_{eq} proves to be the most decisive for system efficiency. In the analyzed range, variations of up to 6% are reached when computing the efficiency.

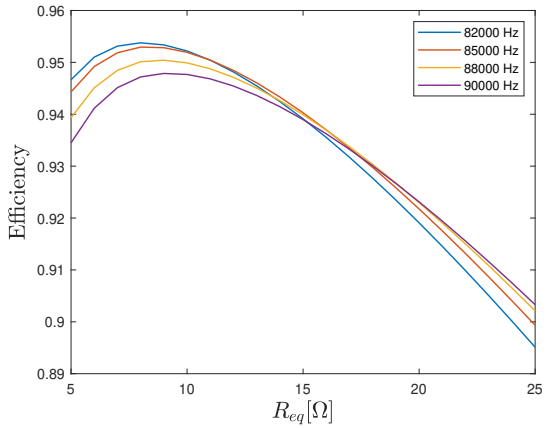

Fig. 3. Evolution of efficiency as a function of R_{eq} and frequency.

IV. Control Design

Predictive controls can be classified in several categories [28]. Within this classification, the Model Predictive Control (MPC) stands out. The operation is based on the development of an accurate model to predict the behavior of the system variables. For the evaluation of the behavior, a cost function is used. This cost function allows the inclusion of non-linearities and operation restrictions, which can model realistic behaviours. This optimization approach seeks to minimize the cost function to obtain the convenient operating points of the system with a fast and stable response.

MPC can be further classified into Continuous Control Set MPC (CCS-MPC) and Finite Control Set MPC (FCS-MPC). The FCS-MPC does not require a modulator because it evaluates each switch position of the converters, but it works with non-fixed frequency. On the other hand, the CCS-MPC requires a modulator and works with a fixed frequency. Setting a fixed frequency is an advantage because the system must operate within the frequency range permitted by regulation. It also simplifies the computation of the compensation system. Thus, the proposed protocol is a CCS-MPC with efficiency as the cost function and multiple testings with different frequencies.

The controller is installed on the primary side but takes measurements from the secondary side. The controller also configures the power converters on both sides. For the acquisition of the measurements and the configuration of the power converters, the controller relies on a wireless communication channel.

One of the controller requirements is knowing the mutual inductance of the coils. This parameter is not a constant in different charger processes as it depends on the relative position between the two coils. To estimate M, a low-current I_1 is applied on the primary side with the secondary side working in an open-circuit state, in a similar way to [30]. With this strategy, computations and measurements are simpler than the ones involved in a closed circuit. In addition, the errors due to the assumption of the component nominal values are avoided. To make this happen, the system includes a contactor on the secondary side. The contactor is normally open and this makes it possible to add an additional safety measure in addition to measuring the open-circuit voltage. The open-circuit voltage measurement (V_2^{oc}) is sent to the primary side with other parameters of the secondary side, such as the self-inductance and the value of the capacitor. This last value can be stored internally during the manufacturing process.

By sending these parameters, the controller installed on the primary side is able to work with a wide variety of power receivers even under non-designed conditions. Once the information is received, the primary controller computes M according to Eq. (9).

$$M = \frac{|V_2^{oc}|}{\omega\,|I_1|} \tag{9}$$

This value, in addition to the reference charging power and the parameters of primary and secondary components, is used by an optimization algorithm. The algorithm computes the optimal operating point of the system to reach the maximum efficiency objective. The solution to the optimization problem provides both the phase-shifting and the operating frequency of the primary inverter. It also defines the duty cycle of the DC/DC converter installed on the secondary side. This solution is used by modulators to operate power electronics.

The optimization problem is defined below. The objective function is the efficiency, as this is the parameter that is expected to be maximized in high-power wireless chargers. To analytically describe this parameter, we first define the equations which include the modelling of the equivalent circuit of both sides of the charger, as well as the power electronic losses and some operation constraints.

The system has been modelled following the generic diagram with SS compensation network depicted in Fig. 2. The equations that model the system are (10) and (11) for the real and imaginary part of the primary side and (12) and (13) for the real and imaginary part of the secondary side when applying Kirchhoff's Voltage Law. The real and

imaginary parts have been analyzed independently because complex numbers are not compatible with most optimization software tools. The primary side includes the MOSFET drain-source on resistance ($R_{m,ds}$), the primary compensation (series capacitor), the resistance and self-inductance of the primary coil and its mutual inductance with secondary coil. In addition to the mutual inductance, the secondary side equations also include the resistance and self-inductance of the secondary coil, the secondary compensation (series capacitor), the diode resistance of the rectifier and the battery equivalent resistance (R_{eq}).

$$(R_1 + 2R_{m,ds})\, ir_1 - \left(\omega L_1 - \frac{1}{\omega C_1}\right) ii_1 - \omega M ii_2 = V_1 \tag{10}$$

$$(R_1 + 2R_{m,ds})\, ii_1 + \left(\omega L_1 - \frac{1}{\omega C_1}\right) ir_1 + \omega M ir_2 = 0 \tag{11}$$

$$-\omega M ii_1 + (R_{eq} + R_2 + 2R_d) ir_2 - \left(\omega L_2 - \frac{1}{\omega C_2}\right) ii_2 = 0 \tag{12}$$

$$\omega M ir_1 + (R_{eq} + R_2 + 2R_d) ii_2 + \left(\omega L_2 - \frac{1}{\omega C_2}\right) ir_2 = 0 \tag{13}$$

Equations (14), (15) and (16) compute the absolute value of the current (im), the phase angle between primary voltage and current (φ_1) and the charging power respectively. It is noted that this last value is a parameter that is adjusted by the user so that our proposed controller ensures a charging power at the maximum efficiency.

$$im_i = \sqrt{ir_i^2 + ii_i^2} \tag{14}$$

$$\varphi_1 = \arctan\left(\frac{ii_1}{ir_1}\right) \tag{15}$$

$$P_{ch} = im_2^2 R_{eq} \tag{16}$$

For a realistic modelling of the system performance, the losses on the power converters should be taken into account. The following equations define MOSFET and diode losses. Equation (17) defines the MOSFET conduction losses ($L_{m,c}$), which are computed using the drain-source on resistance. This value depends on the temperature of the MOSFETs, however, they operate in a stable temperature in steady state, which allows to use a fixed value for the drain-source on resistance. Equation (18) computes the switching losses ($L_{m,sw}$) and they include losses due to the rise and fall times and the output capacitance (C_{oss}). We have set the rise and fall times as their mean values to simplify the equations. Equation (19) corresponds to duty-cycle losses ($L_{m,dt}$). Equation (20) calculates the snubber losses ($L_{m,sn}$). In order to simplify this calculation, a correction parameter (α_{sn}) has been used [34], which is defined by $\alpha_{sn} = 2\frac{R_{sn}C_{sn}}{t_m}\left(1 - \frac{R_{sn}C_{sn}}{t_m}\right)$. Equation (21) groups all the MOSFET losses (L_m). Finally, equation (22) defines the losses of the secondary rectifier (L_d), based on the dynamic resistance of the diodes (R_d). Similar to MOSFETs, this value also depends on the temperature of the diodes but, in steady state, this temperature stabilizes.

$$L_{m,c} = 2im_1^2 R_{m,ds} \tag{17}$$

$$L_{m,sw} = \sqrt{2} V_{in} im_1^2 \sin\varphi_1 t_m \frac{\omega}{2\pi} + 2C_{oss} V_{in}^2 \frac{\omega}{2\pi} \tag{18}$$

$$L_{m,dt} = V_{in} im_1 (1 - D) \tag{19}$$

$$L_{m,sn} = 4C_{sn} R_{sn} \frac{\omega}{2\pi} \alpha_{sn} \tag{20}$$

$$L_m = L_{m,c} + L_{m,sw} + L_{m,dt} + L_{m,sn} \tag{21}$$

$$L_d = 2im_2^2 R_d \tag{22}$$

In order to ensure that the system operates within the operating limits, additional restrictions have been included. Equation (23) restricts the operating frequency to the range defined in RP SAE J2954. Similarly, the equation (24) limits the maximum output voltage of the high-frequency inverter to that of the DC link.

$$\omega \geq \underline{\omega}; \qquad \omega \leq \overline{\omega} \tag{23}$$

$$V_1 \leq \frac{2\sqrt{2} V_{in}}{\pi} \tag{24}$$

Finally the objective function is defined in (25), which corresponds to the real efficiency (η) of the system. The efficiency is computed dividing the output power by the input power, which corresponds to the charging power and the sum of the relevant losses of the charger, including the losses in the coils, the inverter and the rectifier. The efficiency value has to be maximized with the charging power established by the user and with the previous restrictions by the defined algorithm.

$$max\left\{\eta = \frac{P_{ch}}{im_1^2 R_1 + im_2^2 R_2 + L_m + L_d + P_{ch}}\right\} \tag{25}$$

With the objective function and the constraints (equations (10) to (25)), we use an optimization tool to solve this problem, that is, to obtain the values for the variables α (using eq. (4)), D (using eq. (5)) and ω. As a result, it provides the optimum values for the inverter frequency, the phase-shifting and the duty-cycle of the secondary DC/DC converter. These values are simultaneously available and they are configured in the power converters at the same time.

V. Experimental Validation

In order to validate the proposed control, a 2-kW prototype was built. The prototype complies with the SAE-J2954 requirements. The main features of the prototype are summarized in Table I. Figure 4 shows a photo of the laboratory implementation.

On the primary side, the first component (number 1) is the full-bridge rectifier. The ripple of the output signal is smoothed with a DC-link (number 2). The full-bridge inverter (number 3) has been implemented with Silicon Carbide (SiC) MOSFET in order to comply with the switching frequency and the power levels specified in RP SAE J2954 [10]. Both legs of the inverter are composed of two CREE evaluation boards

TABLE I
CHARACTERISTICS OF THE ANALYZED WIRELESS CHARGER.

Design frequency	85 kHz
Operating frequency [10]	81.39-90 kHz
Primary coil dimensions	0.51 m × 0.66 m
Resistance of the primary coil (R_1)	85.2 mΩ
Self-inductance of the primary coil (L_1)	70.93 μH
Secondary coil dimensions	0.35 m × 0.35 m
Resistance of the secondary coil (R_2)	118.7 mΩ
Self-inductance of the secondary coil (L_2)	47.89 μH
Distance between coils assumed in the design (gd)	0.10 m
Compensation topology	Series-Series
Capacitance of the primary side (C_1)	56.50nF
Capacitance of the secondary side (C_2)	82.83 nF
Battery resistance (R_{batt})	25 Ω
Input voltage of the primary inverter	230 V

KIT8020-CRD-8FF1217P-1. Each board includes two CREE SiC MOSFETS model C2M0080120D as well as the activation and protection circuits (e.g. the snubber circuits). In addition, the boards have a special design to reduce the switching oscillations and, therefore, the ElectroMagnetic Interferences (EMI) [35]. Considering the voltages and the frequency in the system, some polypropylene capacitors are used for the compensation networks (number 5 and 6). Rectangular Coils (in Figure 5) are made of AWG-38 Litz wire with dimensions according to SAE J2954. The coils include ferromagnetic materials and shielding on the secondary side.

On the secondary side, we have the full-bridge rectifier (number 7) and the DC-DC converter (number 8). The rectifier is composed of two CREE evaluation boards with two C4D20120D SiC diodes. The DC-DC converter has been implemented with another C2M0080120D MOSFET and a 20.4 μH coil. Finally, the battery is modelled with an electronic load (number 10).

As for the controllers, both a Raspberry Pi 4 Model B and a dsPIC30F4011 have been used on the primary and secondary sides (numbers 4 and 9). Raspberry is a low-cost single-board computer with WiFi and Bluetooth connectivity. It allows for an ARM executing environment. For this prototype, the controller has been programmed using Python and the Bluetooth connection has been configured.

Once the vehicle is detected, the process starts with the estimation of the mutual inductance. To do so, a great phase-shifting is configured for the inverter so that a low 85-kHz signal is generated. The secondary side is adjusted to operate as an open circuit with the contactor S_i. Then, the open-circuit voltage is sampled. Measuring this voltage is complex due to the high frequency of the signal. This operation is performed by a True RMS-to-DC Converter model AD736 from Analog Devices. With this device, the voltage can be measured with high precision using an analog to digital converter (ADC). For our implementation, the value of the estimated M is 18.9 μH. The coils are separated 10 cm.

The primary controller receives this information from the secondary side using the Bluetooth connection and it computes the mutual inductance according to Equation 9. This parameter and the rest of the system parameters are used to complete the optimization problem. The optimization model has been built using the GEKKO Optimization Suite [36] and solved using IPOPT [37], which requires less than 0.1 seconds to reach the solution.

The result of the optimization problem provides the operation references for the primary inverter and the secondary DC/DC converter all together. These configuration parameters are concurrently programmed in the controllers of the power converters.The primary inverter is operated by the dsPIC, a 16-bit microcontroller of the manufacturer MICROCHIP which receives the phase-shift and frequency reference from the Raspberry Pi and operates the power electronics using its output comparison module. The activation signals are sent to the evaluation boards that perform the switching of the MOSFETs by the gate drivers. The duty cycle of the secondary DC/DC converter is sent to the secondary side using the Bluetooth connection.

The equivalent resistance of a battery varies during its charging process. We have conducted tests for different values of the R_L. Table II presents the results of these tests and compare the proposed strategy with two methods: (i) a configuration algorithm that only adjusts the inverter frequency and (ii) a configuration algorithm that works on the phase-shifting but not on the frequency. For a fair comparison, the three methods adjust the secondary DC/DC converter with the same parameters to test the same value for the R_L. This resistance has been fixed to 5, 10 and 15 Ω. The reference power, that is, the value of P_{ch} in Eq. (16) is set to 2 kW. Efficiency is computed by dividing the measured charging power on the battery bus by the input power on the primary DC bus.

The results show that the control algorithm fulfills its functions both to improve the efficiency and to regulate the charging power. Although the algorithm that only adjusts the frequency is capable of improving efficiency, it does not have enough capacity to regulate the charging power because it can only move in the range of frequencies allowed in the regulations. As a consequence, the power delivered to the load exceeds the reference level, which can cause serious electrical damages. The algorithm tuning only the phase-shifting does have this ability to control the charging power over the entire range. However, the inability to control the frequency makes it impossible to reach the efficiencies obtained by the algorithm proposed in this paper.

TABLE II
COMPARISON OF THE PROPOSED CONTROLLER VERSUS SINGLE-VARIABLE CONTROLLERS.

R_L	Algorithm	η (%)	P_{ch} (W)	α	f (kHz)
5 Ω	Proposed	96.6	2000	172	81.8
	Frequency	94.3	2100	180	81.4
	Phase-shifting	92.5	2000	134	85.0
10 Ω	Proposed	96.9	2000	103	83.0
	Frequency	-	4233*	180	81.4
	Phase-shifting	95.7	2000	96	85.0
15 Ω	Proposed	95.6	2000	87	85.4
	Frequency	-	5982*	180	81.4
	Phase-shifting	95.5	2000	87	85.0

* Not Computed value due to excessive power.

For the experiments in Table II, the DC/DC converter was not configured with the optimum parameters. When this

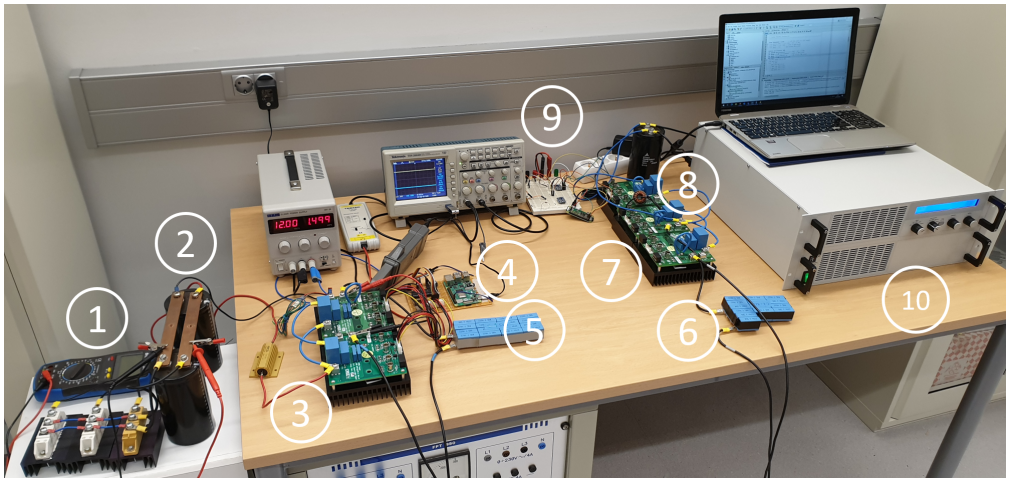

Fig. 4. Power electronics of the implemented prototype.

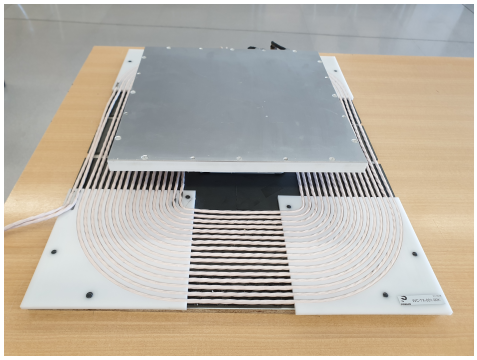

Fig. 5. Picture of both coils with the parameters indicated in Table I.

converter is also adjusted properly, the performance of the controller improves. Table III shows a comparison of optimal operating values for different M values when the DC/DC converter is also configured according to the proposed algorithm. The M values correspond to a vertical separation of 10, 12, and 14 cm, being the centers of both coils aligned. The battery resistance is 25Ω and the charging power is 2 kW. The proposed controller adjusts the duty cycle of the DC/DC converter according to M, leading to different values of R_L. The optimal operating point reveals that R_L should be between 5 and 10 Ω. The frequency adjusted by the algorithm keeps in the lower range allowed by RP SAE J2954. From these results, it can be deduced that the value of M affects not only the optimum efficiency but it also impacts on the recommended operating parameters. In this particular case, the system improves the efficiency by setting a lower equivalent resistance and frequency when the misalignment is reduced M.

Table III also includes a comparison of the proposed controller with other controllers usually employed in the related literature [32]. Every analyzed controller has the ability of adjusting the charging power. The first is a simple PI controller, which adjusts the charging power varying the phase-shift angle of the inverter. We extend previous comparisons [20], [32] by including MEPT controllers. Due to the limitations of MEPT algorithms, they can only control two variables: the phase-shift angle of the inverter to adjust the charging power and the frequency or the equivalent resistance to improve the efficiency. The comparison comprises both implementation of the MEPT controllers.

TABLE III
COMPARISON OF THE EFFICIENCY UNDER DIFFERENT M VALUES.

M (μH)	Algorithm	η (%)	R_L (Ω)	α	D	f (kHz)
18.9E-6	Proposed	97.2	8.5	110	0.42	82.4
	PI controller	94.2	25	80	-	85.0
	R_{eq} MEPT	96.2	8.8	106	0.41	85.0
	Freq MEPT	95.6	25	116	-	89.8
17.1E-6	Proposed	95.9	7.5	104	0.45	82.1
	PI controller	92.7	25	80	-	85.0
	R_{eq} MEPT	95.0	7.8	99	0.44	85.0
	Freq MEPT	94.5	25	128	-	89.8
14.9E-6	Proposed	95.1	6.3	97	0.50	81.8
	PI controller	90.7	25	84	-	85.0
	R_{eq} MEPT	94.5	6.7	90	0.48	85.0
	Freq MEPT	92.4	25	180	-	90.0

As demonstrated by the theoretical analysis in Section III, reaching the optimum operation point requires the configuration of the three configuration parameters. Thus, the PI controller presents the lower efficiency because it operates with the battery equivalent resistance and the nominal frequency without adjusting them. MEPT algorithms improve this efficiency, but specifically the controller which adjusts the battery equivalent resistance reaches higher efficiency values than the frequency MEPT controller because currents (and the associated losses) are lower on primary and secondary sides. Finally, the proposed algorithm manages the highest efficiency values under any M value.

Figure 6 shows the voltage and current measurements of the primary and secondary sides respectively for optimal operation with 18.9 μH of mutual inductance. These measurements show a slight gap between the voltage and current signals, due to the impossibility of using ideal capacitors and the exact frequency proposed by the optimization problem. One relevant feature of MPC is its capability to provide a fast and damped

transient response. In our implementation, for a R_{batt} equal to 25 Ω and a reference power of 2 kW, the transient of the secondary DC signal was 125 ms, which is appropriate for static wireless chargers.

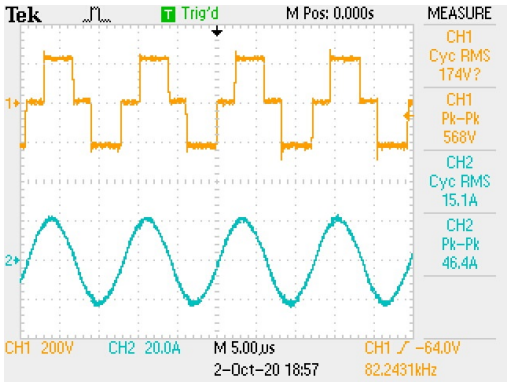

(a) Primary

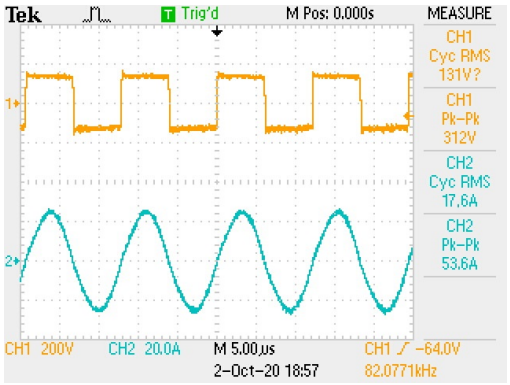

(b) Secondary

Fig. 6. Measurement of primary and secondary voltages and currents.

The prototype complies with the restrictions on electromagnetic emissions defined by the International Commission on Non-Ionizing Radiation Protection (ICNIRP) [38]. In its guidelines for limiting exposure to time-varying electric and magnetic fields, this commission sets two maximum reference levels for the magnetic flux density for the frequency range between 3 kHz-10 MHz: 100 μT for occupational exposure and 27 μT for general public exposure. This prototype reaches its maximum level for a distance equal to zero from the edge of primary coil, with a value of 4.7 μT and a charging power equal to 2 kW. We used an spectrum analyzer Spectran NF-50355 for the measurements.

VI. Conclusion

A novel predictive control to maximize power efficiency for EV wireless chargers has been proposed. The control outperforms other configuration algorithms by adjusting up to three parameters of the power converters. The theoretical analysis has demonstrated that the frequency and the battery equivalent resistance have a real impact on the charging efficiency, while the phase shifting makes it possible to control the charging power.

Based on the circuit model of the system, the charger parameters are introduced into a linear optimization problem. The solution provides optimal values for the operating frequency, the primary voltage and the equivalent resistance in order to ensure maximum efficiency in the power transfer. The control has been validated with a real implementation in a 2-kW prototype. The evaluation results verify that the adjustment of the three parameters leads to an improved power transfer, reaching an efficiency level that is up to 4% greater than when only one of these parameters in the analyzed range is adjusted. The advantage is more notable for low values of R_L, that is, the resistance associated to the load without the effect of the DC/DC converter. The theoretical and experimental analysis shows that the proposed algorithm exhibit a better performance for low values of R_L, which is the region where the system is more efficient. The robustness of the control has also been validated with different values of mutual inductance. The same dependence with R_L has been observed.

The authors plan to continue this research line with two main actions. Firstly, the developed control will be adapted and tested with a real EV battery. We will study how to integrate the prototype with the BMS and if it possible to acquire and use more data from the battery. Secondly, we will design, develop and test a MPC for a bi-directional EV wireless charger in order to get the maximum efficiency in the two-way power flows associated to Vehicle-to-Grid (V2G) operations. A bi-directional charger requires different topologies for the power converters, so new parameters (such as the phase-shifting of the primary and the secondary AC/DC converters) should be configured by the MPC under this configuration.

References

[1] S. S. Williamson, S. M. Lukic, and A. Emadi, "Comprehensive drive train efficiency analysis of hybrid electric and fuel cell vehicles based on motor-controller efficiency modeling," *IEEE Transactions on Power Electronics*, vol. 21, no. 3, pp. 730–740, 5 2006.

[2] BloombergNEF, " Electric Vehicle Outlook 2020," Tech. Rep., 2020. [Online]. Available: https://about.bnef.com/electric-vehicle-outlook/

[3] S. Statharas, Y. Moysoglou, P. Siskos, G. Zazias, and P. Capros, "Factors Influencing Electric Vehicle Penetration in the EU by 2030: A Model-Based Policy Assessment," *Energies*, vol. 12, no. 14, pp. 2739–2763, 7 2019.

[4] A. Trivino-Cabrera, J. M. Gonzalez-Gonzalez, and J. A. Aguado, *Wireless Power Transfer for Electric Vehicles : Foundations and Design Approach*, ser. Power Systems. Springer International Publishing, 2020.

[5] S. Jeong, Y. J. Jang, and D. Kum, "Economic Analysis of the Dynamic Charging Electric Vehicle," *IEEE Transactions on Power Electronics*, vol. 30, no. 11, pp. 6368–6377, 11 2015.

[6] A. Triviño-Cabrera, J. Aguado, and J. M. González, "Analytical characterisation of magnetic field generated by ICPT wireless charger," *Electronics Letters*, vol. 53, no. 13, pp. 871–873, 6 2017.

[7] S. Li and C. C. Mi, "Wireless power transfer for electric vehicle applications," *IEEE Journal of Emerging and Selected Topics in Power Electronics*, vol. 3, no. 1, pp. 4–17, 3 2015.

[8] International Electrotechnical Committee, "IEC TS 61980-3:2019 - Electric vehicle wireless power transfer (WPT) systems - Part 3: Specific requirements for the magnetic field wireless power transfer systems," 2019.

[9] International Organization for Standardization, "ISO 19363:2020(en) Electrically propelled road vehicles - Magnetic field wireless power transfer - Safety and interoperability requirements," 2020.

[10] SAE International, "J2954B: Wireless Power Transfer for Light-Duty Plug-in/Electric Vehicles and Alignment Methodology," 2019.

[11] J. M. González-González, A. Triviño-Cabrera, and J. A. Aguado, "Design and Validation of a Control Algorithm for a SAE J2954-Compliant Wireless Charger to Guarantee the Operational Electrical Constraints," *Energies*, vol. 11, no. 3, pp. 604–620, 3 2018.

[12] B. Vu, J. M. Gonzalez-Gonzalez, V. Pickert, M. Dahidah, and A. Trivino, "A hybrid charger of conductive and inductive modes for Electric Vehicles," *IEEE Transactions on Industrial Electronics*, 2020.
[13] H. Li, J. Li, K. Wang, W. Chen, and X. Yang, "A maximum efficiency point tracking control scheme for wireless power transfer systems using magnetic resonant coupling," *IEEE Transactions on Power Electronics*, vol. 30, no. 7, pp. 3998–4008, 7 2015.
[14] N. Y. Kim, K. Y. Kim, J. Choi, and C. Kim, "Adaptive frequency with power-level tracking system for efficient magnetic resonance wireless power transfer," *Electronics Letters*, vol. 48, no. 8, pp. 4–5, 2012.
[15] C. Özdemir and A. N. Mete, "A Frequency-Tracking Algorithm for Inductively Coupled Wireless Power Transfer Systems," in *10th International Conference on Electrical and Electronics Engineering*, 2017, pp. 1461–1465.
[16] D. Patil, S. Member, M. Sirico, L. Gu, S. Member, and B. F. Fellow, "Maximum Efficiency Tracking in Wireless Power Transfer for Battery Charger : Phase Shift and Frequency Control," *2016 IEEE Energy Conversion Congress and Exposition (ECCE)*, pp. 1–8, 2016.
[17] W. X. Zhong and S. Y. Hui, "Maximum energy efficiency tracking for wireless power transfer systems," *IEEE Transactions on Power Electronics*, vol. 30, no. 7, pp. 4025–4034, 7 2015.
[18] Y. Narusue, Y. Kawahara, and T. Asami, "Maximum efficiency point tracking by input control for a wireless power transfer system with a switching voltage regulator," in *IEEE Wireless Power Transfer Conference*. Institute of Electrical and Electronics Engineers Inc., 6 2015.
[19] H. H. Wu, A. Gilchrist, K. D. Sealy, and D. Bronson, "A high efficiency 5 kW inductive charger for EVs using dual side control," *IEEE Transactions on Industrial Informatics*, vol. 8, no. 3, pp. 585–595, 2012.
[20] Z. Zhou, L. Zhang, Z. Liu, Q. Chen, R. Long, and H. Su, "Model Predictive Control for the Receiving-Side DC-DC Converter of Dynamic Wireless Power Transfer," *IEEE Transactions on Power Electronics*, vol. 35, no. 9, pp. 8985–8997, sep 2020.
[21] Z. Huang, C. S. Lam, P. I. Mak, R. P. D. S. Martins, S. C. Wong, and C. K. Tse, "A Single-Stage Inductive-Power-Transfer Converter for Constant-Power and Maximum-Efficiency Battery Charging," *IEEE Transactions on Power Electronics*, vol. 35, no. 9, pp. 8973–8984, 9 2020.
[22] J. Y. Lee and B. M. Han, "A bidirectional wireless power transfer EV charger using self-resonant PWM," *IEEE Transactions on Power Electronics*, vol. 30, no. 4, pp. 1784–1787, 4 2015.
[23] X. Dai, X. Li, Y. Li, and A. P. Hu, "Maximum Efficiency Tracking for Wireless Power Transfer Systems with Dynamic Coupling Coefficient Estimation," *IEEE Transactions on Power Electronics*, vol. 33, no. 6, pp. 5005–5015, 2018.
[24] J. Vázquez, P. Roncero-Sánchez, and A. Parreño Torres, "Simulation Model of a 2-kW IPT Charger with Phase-Shift Control: Validation through the Tuning of the Coupling Factor," *Electronics*, vol. 7, no. 10, p. 255, 10 2018.
[25] L. Murliky, R. W. Porto, V. J. Brusamarello, F. Rangel de Sousa, and A. Triviño-Cabrera, "Active Tuning of Wireless Power Transfer System for compensating coil misalignment and variable load conditions," *AEU - International Journal of Electronics and Communications*, vol. 119, p. 153166, may 2020.
[26] M. Shadmand, R. S. Balog, and H. Abu Rub, "Maximum Power Point Tracking using Model Predictive Control of a flyback converter for photovoltaic applications," in *Power and Energy Conference*. Institute of Electrical and Electronics Engineers (IEEE), 5 2014, pp. 1–5.
[27] A. Laib, F. Krim, B. Talbi, A. Kihal, and A. Sahli, "Predictive control strategy for double-stage grid connected PV systems," in *Lecture Notes in Electrical Engineering*. Springer Verlag, 11 2019, vol. 522, pp. 314–327.
[28] S. Kouro, P. Cortes, R. Vargas, U. Ammann, and J. Rodriguez, "Model Predictive Control - A Simple and Powerful Method to Control Power Converters," *IEEE Transactions on Industrial Electronics*, vol. 56, no. 6, pp. 1826–1838, 6 2009.
[29] P. Cortés, M. P. Kazmierkowski, R. M. Kennel, D. E. Quevedo, and J. Rodriguez, "Predictive control in power electronics and drives," *IEEE Transactions on Industrial Electronics*, vol. 55, no. 12, pp. 4312–4324, 2008.
[30] A. A. S. Mohamed and O. Mohammed, "Bilayer Predictive Power Flow Controller for Bidirectional Operation of Wirelessly Connected Electric Vehicles," *IEEE Transactions on Industry Applications*, vol. 55, no. 4, pp. 4258–4267, 7 2019.
[31] C. Qi, Z. Lang, L. Su, X. Chen, and H. Miao, "Model predictive control for a bidirectional wireless power transfer system with maximum efficiency point tracking," in *IEEE International Symposium on Predictive Control of Electrical Drives and Power Electronics*. Institute of Electrical and Electronics Engineers Inc., 5 2019.
[32] S. Liu, R. Mai, L. Zhou, Y. Li, J. Hu, Z. He, Z. Yan, and S. Wang, "Dynamic Improvement of Inductive Power Transfer Systems with Maximum Energy Efficiency Tracking Using Model Predictive Control: Analysis and Experimental Verification," *IEEE Transactions on Power Electronics*, vol. 35, no. 12, pp. 12 752–12 764, dec 2020.
[33] W. Li, H. Zhao, J. Deng, S. Li, and C. C. Mi, "Comparison Study on SS and double-sided LCC compensation topologies for EV/PHEV Wireless Chargers," *IEEE Transactions on Vehicular Technology*, vol. 65, no. 6, pp. 4429–4439, 2016.
[34] N. Rosseti and R. Lan, "Correct Snubber Power Loss Estimate Saves the Day," San Jose, CA, USA, 2016.
[35] "Silicon Carbide MOSFET Evaluation Kit, KIT8020CRD8FF1217P-1 datasheet," CREE.
[36] L. Beal, D. Hill, R. Martin, and J. Hedengren, "GEKKO Optimization Suite," *Processes*, vol. 6, no. 8, p. 106, 7 2018.
[37] A. Wächter and L. T. Biegler, "On the implementation of an interior-point filter line-search algorithm for large-scale nonlinear programming," *Mathematical Programming*, vol. 106, no. 1, pp. 25–57, 5 2006.
[38] International Commission on Non-Ionizing Radiation Protection, "Guidelines for limiting exposure to time-varying electric and magnetic fields (1 Hz TO 100 kHz)," *Health Physics*, vol. 99, no. 6, pp. 818–836, dec 2010.

Jose M. González-González was born in Málaga, Spain. He received the M. degree in industrial engineering from University of Málaga, Spain in 2015.

He is currently working towards a Ph.D. on wireless power transfer in electric vehicles, focused on the design of a prototype with bi-directional features. He also has practical experience working on smart grids and renewable energy projects, with some publications on the integration of battery energy storage.

Alicia Triviño-Cabrera was born in Málaga, Spain. She received the M. degree in telecommunication engineering and computer science engineering from University of Málaga, Spain in 2002 and 2008 respectively. Her Thesis, which was defended in 2007, focused on wireless networks.

She currently holds a position as an Associate Professor at the University of Málaga. Since 2011, her research activities focus on wireless power transfer. In the area related to Electric Vehicles wireless chargers, she has actively participated in the design and development of three prototypes including features as bi-directionality and dynamic charge.

José A. Aguado (M'01) was born in Málaga, Spain. He received the electrical engineer and Ph.D. degrees from the University of Málaga, Málaga, Spain, in 1997 and 2001, respectively.

He is a Full Professor and Head of the Electrical Engineering Department, University of Málaga, Spain. He has led more than 40 publicly funded research and consulting projects on the operation and planning of smart grids and wireless power transfer.